TU
WIEN

TECHNISCHE
UNIVERSITÄT
WIEN
Vienna University of Technology

DIPLOMA THESIS

Ranging precision of an existing UWB transceiver with a custom designed antenna

supervised by

Univ.Prof. Ing. Dipl.-Ing. Dr.-Ing. Christoph F. Mecklenbräuker
and
Senior Scientist Dipl.-Ing. Dr.techn. Robert Langwieser

performed at the
Institute of Telecommunications

by

Dragomir Chingov
Matr.Nr. 1028394
Boschstrasse 24/6/1, 1190 Vienna

Vienna, 11.November.2016

DIPLOMARBEIT

Genauigkeit der Abstandsmessung mittels eines existierenden UWB Transceivers mit einer eigenes entworfenen Antenne

von

Dragomir Chingov
Matr.Nr. 1028394
Boschstrasse 24/6/1, 1190 Wien

Wien, 11.November.2016

ABSTRACT

In this Master thesis the ranging accuracy of an off-the-shelf commercial, IEEE 802.15.4 – 2011 Low-Rate Wireless Personal Area Network (LR-PAN) compatible ultra-wideband (UWB) transceiver and the influence of an UWB antenna on its' precision is evaluated through measurements. As such, the transceiver's requirements were analyzed to find a suitable match for an antenna realization. Main purpose of the transceiver-antenna system is focused on range estimation through a two-way ranging (TWR) algorithm, by means of free-space time of flight (TOF) calculation. From the measurements it is observed how accurate the range estimate is, with respect to effects, caused by different types of antennas. Chapter 1 introduces a historical overview of ultra-wideband - its definitions and spectral requirements, proposed by the European regulation body. A summary of the IEEE 802.15.4 – 2011 standard alongside with specifications of the selected transceiver system and relation to the antenna design are described in Chapter 2. Discussions about the choice of the designed UWB antenna type and its specifics, regarding the range measurements are given in Chapter 3. Finally, the designed antenna has been tested with the UWB transceiver for the purpose of range estimation and the measured results, which are discussed in Chapter 4.

KURZFASSUNG

Die aktuelle Masterarbeit evaluiert der Reichweitegenauigkeit eines kommerziellen, IEEE 802.15.4 - 2011 Low-Rate Wireless Personal Area Network (LR-PAN) kompatiblen Ultrabreitbandigen-Transceivers und der Einfluss einer Ultrabreitbandantenne. Es wurden die Transceiver-Anforderungen berücksichtigt, um eine passende Antenne dafür zu realisieren. Der Hauptzweck des Transceiver-Antennensystems ist die Reichweiteschätzung, anhand eines „Two-Way Ranging"-Algorithmus, mittels Berechnung der Verzögerungszeiten im freien Raum. Aus den Entfernungsmessungen wird statistisch ermittelt, welche Genauigkeit die Entfernungsschätzung in Abhängigkeit von Antenneneinflüssen ist. Kapitel 1 stellt einen historischen Überblick des Begriffs Ultrabreitband - seine Definitionen und die von den Europäischen-Regulatorbehörden vorgeschlagenen spektralen Anforderungen dar. Eine Zusammenfassung des IEEE 802.15.4 – 2011 Standars, die Spezifikationen des ausgewählten Transceivers und seine Antennenanforderungen sind in Kapitel 2 zusammengefast. Die Diskussionen des entworfenen ultrabreitbandigen Antennentyps und seine Besonderheiten in Bezug auf die Entfernungsmessungen werden in Kapitel 3 angegeben. Anschließend wurde die Reichweitegenauigkeit, anhand der entworfenen Antenne im Zusammenhang mit dem UWB-Transceivers getestet und die Ergebnisse davon in Kapitel 4 zusammengefasst.

Table of Contents

LIST OF ABBREVIATIONS

MAC - Media Access Control

OSI - Open Standard Interconnect

UWB - Ultra-wideband

FCC - Federal Communications Commission

PPDU - Physical Protocol Data Unit

SHR - Synchronization header

SFD - Start of Frame delimiter

PHR - Physical header

BPSK - Binary Phase-shift keying

BPM - Burst-position modulation

EVK - Evaluation kit

EVB - Evaluation board

SPI - Serial Peripheral Interface

TWR - Two-way ranging

EIRP - Equivalent Isotropically Radiated Power

CPW - Coplanar waveguide

LOS - Line-of-sight

CRC - Cycle redundancy check

FSPL - Free-space path loss

PRF - Pulse repetition frequency

CHAPTER 1: Introduction

In the middle of 1990, a review panel at the Defense Advanced Research Projects Agency (DARPA) made an assessment of short impulse signals, which have very wide bandwidth, exploring their potential application, with focus on radars [1]. This panel came up with the definition of so called ultra-wideband (UWB) signals, which are bandwidth specified, with respect to (w.r.t.) spectral power, where the fractional bandwidth (B_f) Eq. (1.1) must be lower bounded by 25%

$$B_f = \frac{BW}{f_c},\qquad(1.1)$$

where f_c and BW are the center frequency and the double-sided bandwidth at the -3dB level, respectively [2].

The following chapter presents a short historical review of the UWB standardization, regulation specifications, and a summary of state of the art.

1.1 Historical background

In the decade after the DARPA assessment report [1], supporters of UWB technology have claimed, that there is also a niche for such a technology in commercial consumer products. According to Shannon's Channel Capacity Theorem, Eq. (1.2), the channel capacity is monotonically increasing with the channel's (or system) bandwidth

$$C = B \, log_2 \left(1 + \frac{P}{N_0 B}\right),\qquad(1.2)$$

where C, B, P, and N_0, are the channel capacity, the bandwidth, the received signal power, and the noise spectral density, respectively. Note, however, that the bandwidth B

enters Eq. (1.2) twice, i.e. a larger bandwidth allows a higher data rate to be transmitted without errors, although this also increases the received noise power N_oB. There is an initial fast increase in channel capacity w.r.t. bandwidth, which saturates to an upper bound – meaning that too much increase in bandwidth does not result in a benefit in capacity [3].

Two effects are important for the understanding of UWB signal and transmission properties. When the transmitted signal bandwidth is very high, the signal power is distributed over a very large frequency band. This offers the possibility of frequency diversity at the receiver. In the case of a rich multipath propagation environment, numerous fading dips occur in the propagation channel, but only a very small portion of the overall signal power is actually lost in the fading dips [4]. Signals of short duration result in signals with very high signal bandwidth. A short signal duration in the time domain offers the possibility to realize sensor systems with a high spatial resolution. This is beneficial for ranging applications.

On the downside, the opponents of UWB are against the license-free operation and "interference" caused by any wideband system, especially within those portions of the spectrum that has been paid for. An example of a legacy service, which might be affected by the interference from large-scale use of UWB transmissions, is the Global Positioning System (GPS): due to its low power receive signal level, the service could be significantly impaired [5].

Federal Communications Commission (FCC) definition

At the beginning of the current century, the FCC adopted a revision to its Code of Federal Regulations, specifically to Part 15 (Title 47 CFR 15), where it permitted the use of UWB capable devices without a license fee. FCC Part 15 of the Federal Regulations encompasses a set of regulations for devices considered as unintentional radiators, e.g. any device that is not deliberately designed to emit radio waves or radiates outside of its intended spectrum. Their electromagnetic emission is not their main application, but rather can be considered as a side effect or a by-product. Despite having the same spectral emission, UWB devices are considered intentional radiators, according to the rules of FCCs Part 15.

Several months later, the revision was released as a First Report and Order, allowing unlicensed transmission on the frequency band from 3.1 to 10.6 GHz offering 7.5 GHz of bandwidth. Detailed emission power limitations and bandwidth constraints were specified for the use of that spectrum. The allowed transmit power spectral density is upper bounded by -41.3 dBm/MHz for this frequency band. This upper bound is intended for protection of legacy services and scientific, and industrial use already occupying many parts of the frequency band [6].

Compared to the DARPA definition, the FCC loosens the conditions under which a signal is considered UWB. An literal excerpt from the FCC Part 15 Section F definition states:

"*(a) UWB bandwidth. For the purpose of this subpart, the UWB bandwidth is the frequency band bounded by the points that are 10 dB below the highest radiated*

emission, as based on the complete transmission system including the antenna. The upper boundary is designated f_H and the lower boundary is designate f_H. The frequency at which the highest radiated emission occurs is designated f_C.

(b) Center frequency. The center frequency, f_C, equals $(f_H + f_L)/2$.

(c) Fractional bandwidth. The fractional bandwidth equals $2(f_H - f_L)/(f_H + f_L)$.

(d) Ultra-wideband (UWB) transmitter. An intentional radiator that, at any point in time, has a fractional bandwidth equal to or greater than 0.20 or has a UWB bandwidth equal to or greater than 500 MHz, regardless of the fractional bandwidth." [7]

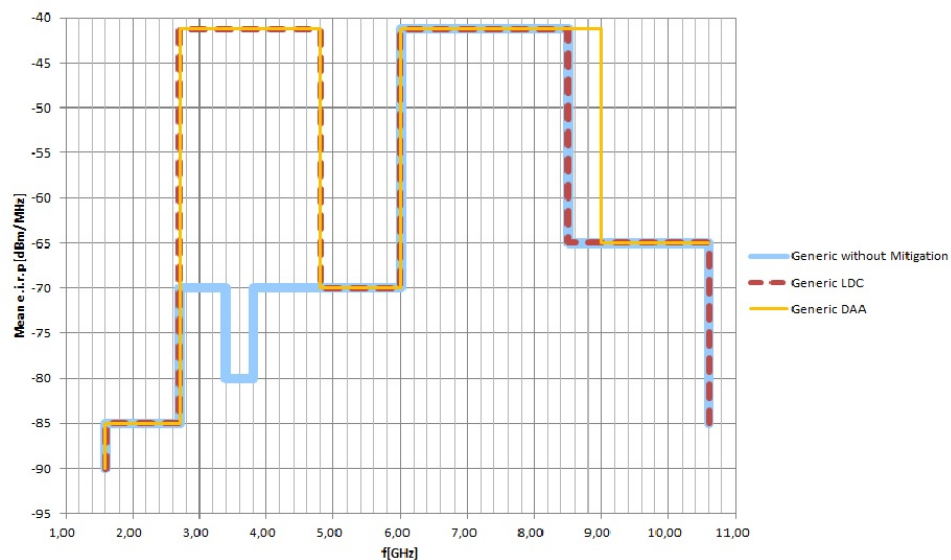Unless stated otherwise in this master thesis, the term *bandwidth* follows the FCC definition.

Figure 1.1 Proposed spectral mask for indoor location service by an ETSI Technical Report [8]

1.2 Spectral Regulation in the EU

In the European Union (EU), the European Telecommunications Standards Institute (ETSI) is one of the bodies defining common system standards and the associated spectral allocation options, also for the use of UWB signals (Figure 1.1). It has imposed spectral constraints, which deviate from the FCC's spectral mask limit of -41.3 dBm/MHz. Since UWB systems must coexist with legacy services that have frequency bands assigned to them exclusively, a mitigation method must be used for the license-free UWB operation not to intervene with the so-called "primary service user".

Mitigation in form of Dynamic Spectrum Access (DSA) techniques such as Detect and Avoid (DAA) and Low Duty Cycle (LDC) must be applied to achieve such protection. DAA is a spectral overlay method, where the secondary user (UWB) may access the spectrum, when the primary user is not simultaneously using it. If the primary user is present, the secondary user must lower its power level accordingly.

LDC, however, uses an underlay scheme where the UWB user transmits simultaneously with the primary user of the licensed band, but with a much lower duty cycle. For example, the ETSI proposal for LDC allows a maximum of 25 ms continuous transmission and a maximum of 5% for a given transmitter for 1s, and at most 1.5 % transmission time per minute [8].

This master thesis focuses on the indoor ranging service. It does not cover other UWB services referred to in the ETSI Technical Report [8] such as data communications,

ground penetrating radar, through-wall imaging systems, or automotive radar applications.

1.3 State of the art

The use of UWB for short range services, under Tx power constraints is a promising workaround to the myriad of wired household solutions. Technology initiatives like the "WiMedia Alliance" and the "UWB Forum" have considered concepts like Multi-Band Orthogonal Frequency-Division Multiplexing (MB-OFDM) and Direct Sequence–UWB (DS-UWB), respectively, allowing high-bandwidth communication over short distance. Unfortunately these concepts did not flourish as expected.

A different approach towards UWB signal application finds its realization in the increasingly demanding market for indoor localization. Having high temporal resolution, UWB Impulse radio (UWB IR) is qualified as a suitable candidate for high precision range estimation. Its competitors are indoor localization solutions such as Wi-Fi [9], Bluetooth [10] or ZigBee [11], which are based on power measurement, or Receive Signal Strength Indication (RSSI). On the other hand, UWB IR signals can be exploited to its advantage where required: localization applications for warehousing or crowded venues, or object tracking at sports events, to name a few:

- In the modern market analysis, understanding of the behavior of the customer inside the store, gives a cutting edge advantage, where every brand on the shelf is looking for recognition. Moreover, 76% of the decisions, whether to buy a product are made inside the store [12].

- The decision, who is going to win a sports match, between high-class competitive teams, can be influenced by the number of referee mistakes. For example, a forward pass in rugby or the ball, passing completely the goal line in a football game, not covered by the match officials.

- Even, tracking the individual athlete in a closed stadium, where GPS is not applicable.

- In the medical industry for patient localization, wireless vital signs monitoring, such as covering respiratory patterns or heart movement and internal organs imaging.

In those applications, location precision of better than 0.5m is not feasible. Some sources even claim that indoor localization will have a larger economic impact than GPS [13]. The following chapters evaluate the performance of an IEEE 802.15.14 – 2011 compliant UWB transceiver, where the term UWB is used instead of IR UWB, as the impulse radio application is the main focus of the current paper.

In short, UWB signals for commercial communication have the following characteristics:

- low-power signal, ergo transmission is intended only for short distances

- larger channel capacity due to larger bandwidth

- high time-domain resolution suitable for high precision localization and localization applications

- multipath fading resilience due to large frequency diversity

CHAPTER 2: UWB transceiver

After presenting the historical development and state of the art, the following chapter introduces the Institute of Electrical and Electronics Engineers (IEEE) 802.4.15 – 2011 standard [14]. It also describes the commercial product chosen for the experiments and measurement evaluation. Being a standard-conformant commercial device, it is possible to measure its ranging capabilities and precision. At the end, the algorithm, implemented for the range estimation is described followed by a summary of the antenna requirements for the UWB transceiver of choice.

2.1 The IEEE 802.4.15 – 2011LR - WPAN standard

Part 15.4 of the IEEE 802 standard focuses on inexpensive, scalable, low-power devices for Low-Rate Wireless Personal Area Networks (LR-WPANs), communicating at distances ranging between several centimeters till the personal operating space of 10m. Each such device has its own unique Media Access Control (MAC) 64-bit address.
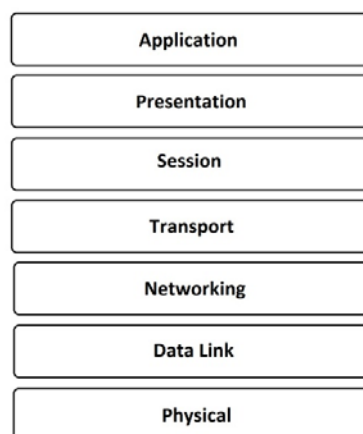

Figure 2.1:   Open Standard Interconnect (OSI) Reference Model

Because of the smaller spatial domain of coverage, WPANs require little or in some cases no infrastructure, compared, with WLANs for example. The standard encompasses the Media Access Control (MAC) sub layer of the Data Link layer and the Physical layer of the Open System Interconnect (OSI) model (Figure 2.1). The current sub-chapter focuses on the Physical layer w.r.t. the spectral requirements and modulation format.

2.1.1 UWB Protocol Data Unit and Modulation

The data communication between nodes takes place by exchanging physical protocol data units (PPDU), referred as UWB frames (Figure 2.2).

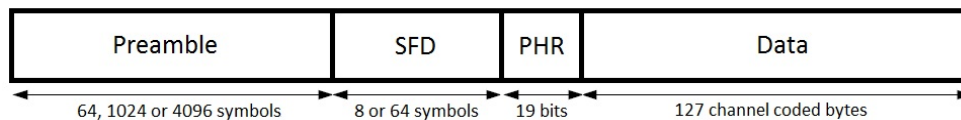| Preamble	SFD	PHR	Data
64, 1024 or 4096 symbols	8 or 64 symbols	19 bits	127 channel coded bytes

Figure 2.2: IEEE 802.15.4 – 2011 PPDU

Transmission of such a frame begins by, first sending a preamble part, which contains a standard predefined pattern code or sequence of pulses. The standard preamble lengths are 64, 1024 and 4096, where each length represents a different number of repetitions of the same pattern code. The preamble ends with a Start of Frame Delimiter (SFD), both of which combine the Synchronization Header (SHR). The preamble codes of the SHR are a sequences of pulses having positive, negative or "zero" value, i.e. no pulse gets transmitted. What follows is the physical header (PHR) which is a 19 bit defined field.

9

The PHR is carrying the information about the data rate, duration of preamble, length of the actual transmitted data and Hamming code parity bits.

Figure 2.3:   SHR followed by PHR – change of modulation format (measured on the output of an EVB1000, see section 2.2)

The PHR also holds an additional, very important meaning during the communication. The time point at which the first symbol of the PHR is transmitted or received is referred to as the timestamp marker.
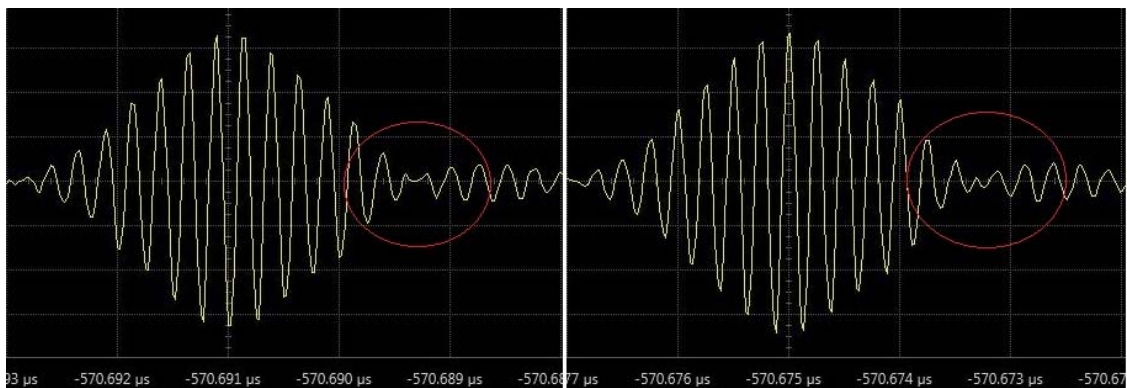

Figure 2.4:   Zoomed in comparison of the phases of two UWB burst at operational band #2 (measured on the output of an EVB1000, see section 2.2)

The transmitter or receiver uses the timestamp in order to calculate the time it takes for the first PHR symbol to be transmitted to the point at which it gets received. Assuming free-space propagation of the transmitted burst and considering the speed of light, the time it takes to receive the PHR can be used to calculate the range.

Unlike the SHR, the PHR and the data are using a burst position modulation (BPM) in conjunction with binary phase shift keying (BPSK) modulation scheme. The resulting symbols are composed of bursts of UWB pulses. The switch from the preamble to the BPM/BPSK modulation is visualized in Figure 2.3. Each BPM/BPSK transmitted symbol has a period T_{dsym}, which is divided into two BPM subintervals, where $T_{BPM} = T_{dsym}/2$. Additionally, the symbol period is represented by an integer number of short pulse (chip) durations $T_{dsym} = N_C T_C$, where N_C is the number of possible chip positions and T_C is the duration of a single chip. By consecutively transmitting N_{cpb} number of chips, a burst pulse is formed with a duration $T_{burst} = N_{cpb} T_C$. The burst is transmitted during either of the symbol halves T_{BPM} and by this way carries the information of bit $b_0^{(k)}$. The information of $b_1^{(k)}$ is carried by the burst polarity (Figure 2.4).

$$y(t)^{(k)} = \left(1 - 2\,b_1^{(k)}\right) \sum_{n=1}^{N_{cpb}} \left(1 - 2\,s_{n+kN_{cpb}}\right) p(t - b_0^{(k)} T_{BPM} - h^{(k)} T_{burst} - nT_c), \tag{2.1}$$

where $s_{n+kN_{cpb}} \in \{0, 1\}, n = 0, 1, \ldots, N_{cpb} - 1$ is the interference rejection polarity scrambling sequence, which introduces additional interference suppression among UWB receivers, $h^k \in \{0, N_{hop} - 1\}$ is the time hopping scheme and $p(t)$ is the transmit pulse. The transmitted pulse $p(t)$ is constrained by the magnitude of its cross-correlation

11

function with a standard defined root-raised cosine reference pulse. For a standard compliant transmitter the cross-correlation magnitude main lobe must have an envelope greater than or equal to 0.8 for a certain standard defined duration and any side lobes must be lower than 0.3.

In total, only $N_{hop} = N_{burst}/4$ burst positions are available for a possible hopping scheme, so the burst duration must be much smaller than half the symbol duration $T_{burst} \ll T_{BPM}$, where the transmission takes place only during the first half of each T_{BPM} in order to mitigate inter-symbol interference (ISI) effects and the number of burst durations per symbol is $N_{burst} = T_{dsym}/T_{burst}$.
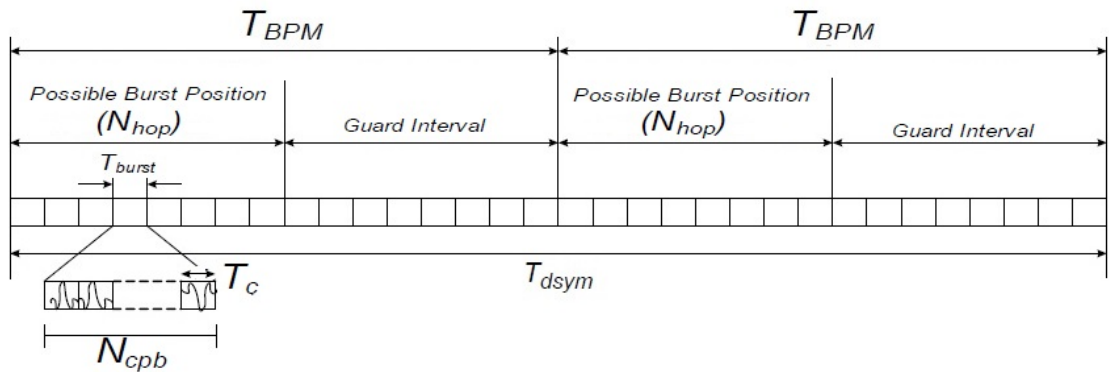

Figure 2.5: UWB symbol period during PHR and Data transmission

2.1.2 Operational bands

The IEEE 802.15.4 – 2011 standard also specifies the so-called operation frequency bands (a.k.a. UWB channels), which are occupied during transmission. On each band, different set of "orthogonal" preambles can be employed - two for a pulse repetition

frequency (PRF) of 16 MHz and four for PRF of 64MHz. By this way multiple users can transmit their preambles on the same channel, without interfering each other. Because of their "perfect" auto-correlation properties, a coherent receiver can estimate the impulse response of the transmission channel, i.e. the preamble sequence symbols are used as pilots or training signals.

Channel number (index)	Pulse duration T_p (in ns)
0, 1, 2, 3, 5, 6, 8, 9, 10, 12, 13, 14	2.00
7	0.92
4, 11	0.75
15	0.74

Table 2.1: Duration (T_p) of the transmit pulse p(t) w.r.t. the IEEE 802.15.4 – 2011

standard operational bands

The IEEE standard, also defines the durations of the transmit pulse *p(t)* (Table 2.1). According to the inverse relation between pulse duration and bandwidth ($T_p = 1/BW$) the bandwidths of the corresponding operational bands (Table 2.2) are compliant with the FCC UWB definition referred in Chapter 1. It should be noted that only channels #0 and #4 comply with the FCC fractional bandwidth definition from Chapter 1, but for all other operational bands the signal bandwidth of 500 MHz and above is considered sufficient. Looking at the power density, however, the IEEE 802.15.4 – 2011 standard defines a limiting spectral mask, where the frequency bounds are

$$\frac{0.65}{T_p} < |f - f_c| < \frac{0.8}{T_p},$$ (2.2)

$$\frac{0.8}{T_p} < |f - f_c|,$$

<div align="right">(2.3)</div>

where inequalities 2.2 and 2.3, correspond to -10dBr and -18 dBr, relative to the center frequency f_c, respectively. The comparison between the bandwidth values listed in Table 2.2 and the spectral mask definition suggests that the actual transmitted power can have a greater bandwidth than the defined, as shown in Figure 2.5. This definition is not to be confused with the regulatory power spectrum requirements mentioned in the introduction.

Band group	Channel number(index)	Center frequency, f_c(MHz)	Bandwidth (MHz)
0	0	499.2	499.2
1	1	3494.4	499.2
	2	3993.6	499.2
	3	4492.8	499.2
	4	3993.6	1331.2
2	5	6489.6	499.2
	6	6988.8	499.2
	7	6489.6	1081.6
	8	7488	499.2
	9	7987.2	499.2
	10	8486.4	499.2
	11	7987.2	1331.2
	12	8985.6	499.2
	13	9484.8	499.2
	14	9984	499.2
	15	9484.8	1354.97

Table 2.2: UWB channel/band allocation

2.2 EVB1000 UWB transceiver

The UWB compatible device, which is evaluated in the current work is a commercial UWB transceiver chip – DW1000 by the company DecaWave Inc. The testbed, evaluated in the current master thesis consists of an evaluation kit (EVK1000) and two sets of UWB antennas. EVK1000 consists of two evaluation printed circuit boards (EVB100) (Figure 2.6).
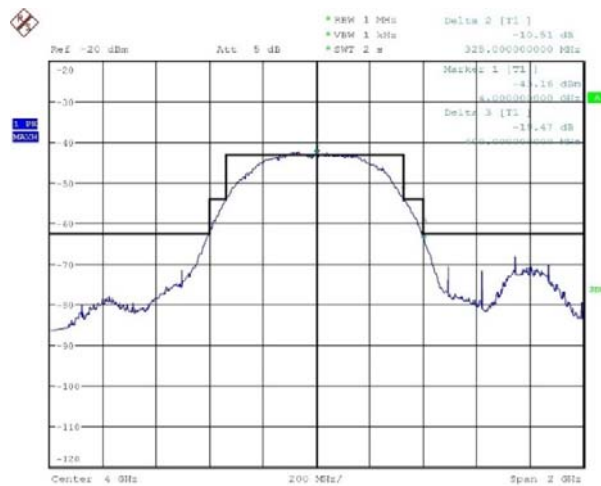

Figure 2.5: Spectral mask of operational band #2 at preamble length of 1024

Each board has a UWB transceiver DW1000 – a CMOS chip, an additional onboard microcontroller, with preprogrammed configuration settings for standalone use and a set of hardware interfaces, e.g. Serial Peripheral Interface (SPI) port for direct UWB chip control, JTAG port for microcontroller access and USB port for USB-to-SPI.

The UWB capable transceiver is the CMOS chip, with a ranging precision presented by the manufacturer of 10 cm. It consists of an analog and digital part, both having a

transmitting and receiving module. The transmitter feeds the encoded data (or bits) to an analog pulse filter. The corresponding impulse response signals are upconverted by a mixer to a synthesizer generated central frequency band, conform to Table 2.2 and amplified before being transmitted [15]. The mixer is used as a gain control in order to adjust the transmit output power, where there is a different gain control when transmitting the SHR and the PHY [16]. When receiving an impulse, it is amplified by a low-noise amplifier and down-converted to baseband. In the baseband it is sampled through an analog-to-digital (ADC) and sent to the digital part for decoding. For the purpose of the range measurements, the USB-to-SPI interface is being used, controlled from a PC evaluation application, which has access to the chip's internal control registers [17].
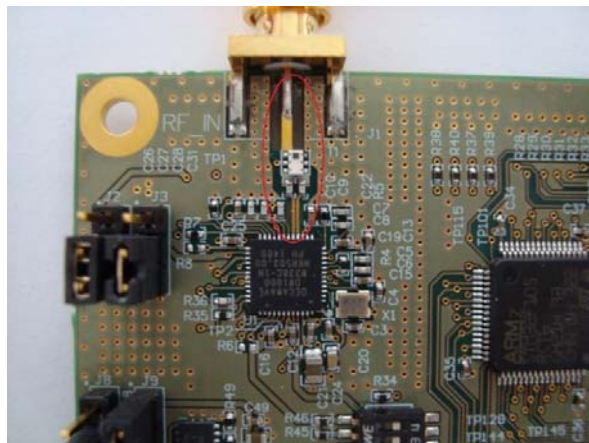

Figure 2.6: Foto of the EVB1000 board showing the radio frequency (RF) feedline

The main purpose of the UWB transceiver is to shift the focus of control from the Physical RF layer to the Data link layer, from the OSI model's perspective, while still being able to configure parameters directly influencing the PDU transmission and its spectral density:

- Bit rate

- Operational band, i.e. center frequency and bandwidth

- Pulse Repetition Frequency

- Preamble length

Nevertheless, the current master thesis examines the performance of the transceiver w.r.t. the Physical layer. The chip supports only the standardized UWB channels #1, #2, #3, #4, #5, #7, but is limited to 900 MHz of bandwidth (Table 2.2) which corresponds to a minimum pulse duration of $T_p = 1.1$ ns.

Additionally, the UWB transceiver supports a set of non-standard features. There are five additional preamble lengths, supported by the UWB transceiver. Also, it is able to change the standard SFD sequence motivated by an increased detection threshold. However, this feature was not investigated in detail in this master thesis.

The evaluation boards are accompanied by a pair of elliptical monopole antennas [18]. In this master thesis, the ranging performance of the elliptical monopole antennas is compared to my bowtie monopole antenna design. This is presented in the following chapter.

2.3 Range estimation algorithm

When using the timestamp to measure the time needed for the first symbol of the PHR from the transmitting node to reach the receiver node, it also measures additional delays, which do not contribute to the actual physical delay between the two endpoints.

2.3.1 Transmitter antenna delay

As depicted from Figure 2.7 the electrical signal passes through several electrical components on its way to its destination - internal chip circuitry, PCB traces, in the case of the EVB1000 implementation, a passive impedance transformer (balun) and the antenna, before being converted into a radiated electromagnetic wave, propagating through the environment. All the delays that do not stem from the wave propagation between the Tx and Rx antenna are referred to cumulatively as "internal delay" or "antenna delay", e.g. t_{ADTX} and t_{ADRX}, for the transmitter and receiver sides, respectively. The internal delay covers the time between the timestamp, at which the first symbol of the PHR leaves the digital part of the chip until the point in time, when it's corresponding signal edge gets radiated by the Tx antenna.
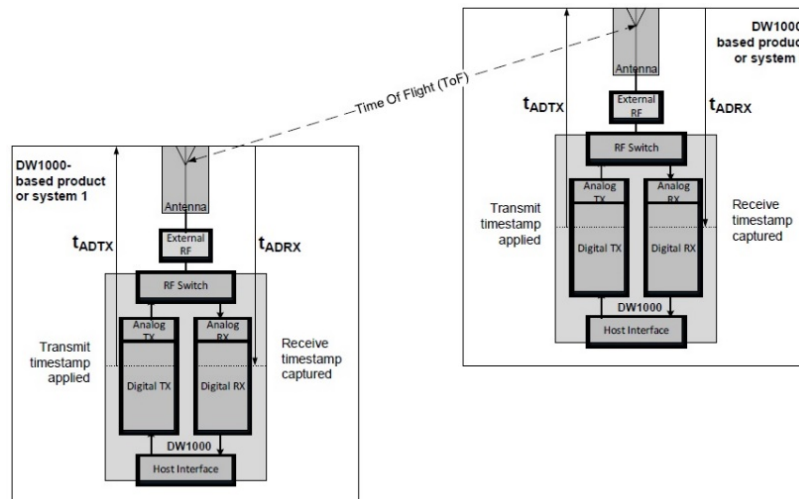

Figure 2.7: Internal delay path (courtesy of Leo Theunissen, decaWave Inc. [19])

The time of flight (TOF) that it takes for the first PHR symbol to travel through the environment from Tx antenna to Rx antenna, is calculated by subtracting the sum of the

antenna delays of both transmitter and receiver, from the total transmission time t_{TOTAL}, see Eq. (2.4).

The UWB transceiver has a separate "Transmitter antenna delay" register that is used to compensate for the aforementioned additional delays (t_{ADTX} and t_{ADRX}) [20]. This whole process of removing the additional antenna delay values is referred to as the delay calibration.

$$ToF = t_{TOTAL} - t_{ADTX} - t_{ADRX} \qquad (2.4)$$

The current thesis investigates primarily this delay calibration. Other types of calibration are not investigated, e.g. power spectrum calibration in terms of the regulatory requirements, or calibration of the crystal oscillator's operating frequency. If not explicitly stated otherwise the term "calibration" refers to delay calibration only.

2.3.2. Two – way ranging (TWR)

The process can be described by a three-way handshake (3-steps), where each transceiver has to have its role assigned. The initiating node is referred to as the Tag and the responding one is called the Anchor. Before the ranging estimation process begins, both Tag and Anchor have to be paired by exchanging their corresponding MAC addresses. The Tag is periodically sending (or "blinking") its MAC address and awaiting a response from an unpaired Anchor, ergo the blinking process. The range measurement uses the timestamp marker of each of the UWB chips and is essentially a three-way handshake algorithm calculating the roundtrip of two messages (Figure 2.8).

The initiator (Anchor) starts by sending a request (polling) to the responding node (Anchor), by noting its send timestamp T_{SP}. Requests are sent on regular intervals until a response is received, within a predefined timeout interval. The responder notes the receive time T_{RP} of the poll and on its behalf sends its own transmit timestamp T_{SR} to the initiator.
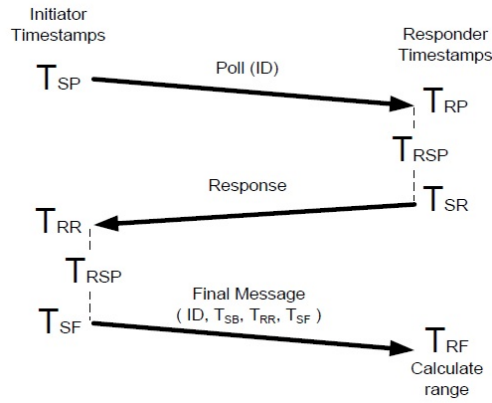

Figure 2.8: TWR roundtrip time diagram (courtesy of Leo Theunissen, decaWave, Inc. [21])

When receiving the response message, the initiator notes the time of reception T_{RR}. After that it delays its transmission in order to be able to send its initial timestamp T_{SP}, the received timestamp of the response T_{RR} and of final response T_{SF} to the responder. The range measurement is performed by two-way ranging (TWR) calculation of equation 2.5.

$$TOF = \left((T_{RR} - T_{SP}) - (T_{SR} - T_{RP}) + (T_{RF} - T_{SR}) - (T_{SF} - T_{RR})\right)/4 , \quad (2.5)$$

with the resulting final information the responder can calculate the round-trip time of the initiator $T_{RR} - T_{SP}$, it calculates its' own response time $T_{RF} - T_{SR}$, subtract the

individual internal processing times $T_{RSP} = T_{SR} - T_{RP}$ or $T_{RSP} = T_{RR} - T_{SF}$ from the previous values and result the TOF, by averaging. The range is calculated by multiplying the TOF value with the speed of light

$$T = \frac{d}{c_0},$$ (2.6)

where d and c_0 is the distance between the approximate phase centers of the Tx and Rx antennas and the speed of light, respectively. In this master thesis, the approximate value for the speed of light in air is $c_0 = 299702547$ m/s [17].

Placing the transmitter and receiver at a known distance and adjusting the internal delay register value, i.e. "Transmitter antenna delay", so that the Time of Flight (ToF) times the propagation speed (c_0) equals the "known distance" Eq. (2.4), (2.6), hides the need to take into account the antenna size and the exact point in space of the antenna phase center, i.e. the effective origin. However, in the case of a dispersive antenna, e.g. a directional antenna, the effective origin depends on the looking angle, so the calibration is done at different angles.

The UWB chips on the EVB1000 boards are delivered with already pre-programmed non-volatile one-time programmable (OTP) memory blocks with corresponding transmit power values. This way the boards are within the transmission power level requirement of -41.3 dBm/MHz.

2.4 Antenna requirements

The RF output of the chip is guided by a 100 Ω differential microstrip line. The differential microstrip line is terminated by a broadband balun which converts the 100 Ω impedance level of the differential line to a 50 Ω impedance single ended line, see Figure 2.6. The balun's 50 Ω terminal feeds the antenna via an SMA (PC 3.5) connector.

The UWB transceiver imposes several requirements on the choice of UWB antenna [22]:

- Matching Requirement: The manufacturer specificies a return loss of more than 10 dB in the desired operational band as a good target value.

- Group Delay Requirement: Recommended are 100 ps (picoseconds) or less for a good ranging precision. According to Eq. (2.6), 100 ps correspond to approx.. 3 cm in propagation distance. This requirement translates into a stringent frequency dispersion limits of the pulse shape.

- Antenna Efficiency Requirements: The manufacturer gives guidelines on acceptable antenna radiation efficiencies. As a rule less than 60% should not be tolerated and 90% is desirable. The antenna efficiency quantifies the disspative losses of the antenna when it converts the RF power at its input into power radiated into the environment.

Depending on the environment and positioning of the antenna, the localization performance will vary. Antennas in proximity to a walls, metal plates, scattering objects of any kind, impairs the ranging performance. In this case a directional antenna might

result in better ranging precision. As shown in the next chapter, there is an argument whether to prefer directional or omnidirectional antennas.

CHAPTER 3: Low band UWB antenna

The antenna is the first and last component on the UWB transmission chain between a wireless source and a sink, which transforms the guided electromagnetic wave into the radiated electromagnetic wave departing from the Tx antenna and vice versa on the Rx side.

This chapter presents a motivation for the choice and the design of a rudimentary UWB antenna solution, suitable for the UWB transceiver presented in Chapter 2 and the challenges that arise due to the large bandwidth requirements.

3.1 UWB antenna theory

What distinguishes UWB from other antennas is its large bandwidth, Eq. (3.1), defined by an upper (f_H) and a lower (f_L) frequency.

$$BW = f_H - f_L \qquad (3.1)$$

A more interesting aspect is what criterion exactly determines the upper and lower frequencies. One might consider bandwidth w.r.t. how much of the radiated energy is directed in a particular direction (antenna directivity - D) or how much of the total transmitted energy is focused in one particular direction (antenna gain - G). The relation between them is referred to as antenna efficiency, which is equivalent to the radiated power (P_{rad}) in relation to the power fed at the input of the antenna (P_{in}) Eq. (3.2).

$$\eta = \frac{P_{rad}}{P_{in}} = \frac{G}{D} \qquad (3.2)$$

Antenna aperture is the term defining the effective surface that encompasses an incoming radiating plane:

$$A = \frac{c_0{}^2 G}{4\pi f^2},$$
(3.3)

where f and c_0 are the frequency and speed of light in vacuum, respectively. Finally, the received power from the receiving antenna is expressed by Friis's law, Eq. (3.4).

$$P_{RX} = \frac{A_{RX}\, A_{TX}\, f^2}{c_0{}^2 r^2}\, P_{TX} = \; G_{RX}\, G_{TX} \left(\frac{c_0}{4\pi d f}\right)^2 P_{TX}\,,$$
(3.4)

where A_{RX} and A_{TX} are the aperture of the receiving and transmitting antenna, d ist the distance between them, f is the frequency, c_0 is the speed of the light in free space, P_{RX} and P_{TX} are the respective receive and transmit powers, G_{RX} and G_{TX} are the respective receive and transmit antenna gains with respect to the isotropic radiator.

With narrowband antennas, the above-mentioned parameters show little variation w.r.t. frequency in their, relatively small operational bands and are considered constant. For UWB antennas this is generally untrue – considering a very large bands, Friis's law becomes frequency dependent, Eq. (3.5) [23].

$$P_{RX} = \int_{-\infty}^{\infty} \frac{G_{RX}(f)\, G_{TX}(f)\, c^2}{f^2 (4\pi d)^2} P_{TX}(f)\, df$$
(3.5)

The large operational bandwidth of an UWB antenna is achievable by multi-scale geometry, where small-scale parts of the radiating elements radiate high frequency components and large-scale parts radiate lower frequency components of the transmitted signal. The frequency response of a temporally short pulse covers a larger part of the

spectrum and its different spectral components "travel" along the antenna through different paths and correspondingly it takes different amount of time to propagate and get radiated. As an example, if we consider an efficient antenna ($\eta \to 1$), according to Eq. (3.2), the gain is, consequently equal to the directivity. Additionally, if the gain and efficiency are constant w.r.t. frequency, than the directivity also stays constant. Constant directivity is rather desirable for UWB, as different frequency components of the transmitted signal are radiated uniformly, which results in minimal temporal dispersion of the signal [24].

If we look at the UWB scenario from the Equivalent Isotropically Radiated Power – EIRP's perspective

$$EIRP = \int_{-\infty}^{\infty} P_{TX}(f)G_{TX}(f)\,df \qquad (3.6)$$

EIRP now becomes the integrated product of gain and power densities. According to the regulatory spectral requirement proposal (Figure 1.1), the EIRP is given constant for a defined frequency range and in order to meet the spectral mask specification, a constant transmit power density is required. As a consequence, from equation 3.3, for a constant gain antenna the aperture is inversely proportional to the square of the frequency ($A \sim 1/f^2$) and with increase of frequency the received energy decreases.

A counterpart of the constant gain is the constant aperture antenna type. Using again the same reasoning from equation 3.3, results in increase of the gain, proportionally to the square of frequency ($G \sim f^2$). Assuming a highly efficient antenna ($\eta \to 1$), if the gain increases with frequency, than correspondingly the directivity decreases, which results in

26

time dispersion of the transmitted signal at frequencies where the directivity gets lower [24].

Since the regulatory requirements do not specify the antenna characteristics explicitly, but rather formulate requirements for the transmitted signal power spectral density, the antenna design should be considered together with transceiver from a systems perspective, rather than separately.

3.2 Bowtie monopole antenna design

Due to the desired low signal dispersion and taking into account the fact that the connector of the UWB transceiver from Chapter 2 is single-ended at its output, a constant gain monopole is the antenna type of choice.
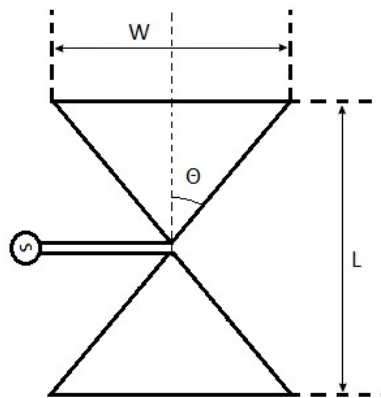
Figure 3.1: Bow Tie Antenna geometry parameters

A possible antenna candidate is chosen by looking back in the history of Oliver Lodge's (1851 – 1940) work, where he extended Heinrich Hertz's (1859 - 1894) fundamental dipole antenna to the biconical dipole. He also considered the 2D approximation to a

planar triangular or bowtie antenna. He postulated that a planar cross-section antenna has comparable parameters to its 3D counterpart. In addition, he recognized that a ground plane (or earth) acts as a symmetry plane w.r.t. the radiating element [25].

The basis of the radiating element is a bowtie antenna model, which is a finite approximation of an infinitely long bowtie antenna and which is intended to be length-independent and instead be parameterized only by an angle value [26]. By selecting the width (W) and length (L) of the bow tie antenna (Figure 3.1) to be a fraction of a desired resonant wavelength, the angle θ becomes the determining factor, see Eq. (3.7) and (3.8) [27] [28].

$$\theta = \arctan\left(\frac{W}{L}\right) \tag{3.7}$$

This approach has the advantage that, since angles are independent of length, the antenna design also becomes wavelength and frequency independent. The antenna impedance Z of an infinitely long biconical dipole antenna becomes

$$Z = \frac{Z_o}{\pi} \ln \cot\left(\frac{\theta}{2}\right), \tag{3.8}$$

where $Z_o \approx 377\ \Omega \approx 120\pi\Omega$ is the free-space wave impedance [26]. The relationship between antenna impedance as a function of the corresponding angle θ is depicted in Figure 3.2, under the assumption that the impedance of a dipole is twice the impedance of its corresponding monopole.

28

3.3 Bowtie monopole antenna simulation and realization

Following Eq. (3.7), the values of W and L have been chosen to be fractions of a desired center wavelength. There are the four operational bands in the low band section of Table 2.2, that are supported by the UWB transceiver in the vicinity of 4 GHz. According to the wavelength – frequency relation w.r.t. propagation speed in free-space, the chosen wavelength is $\lambda_0 \approx 0.075\,\text{m}$.
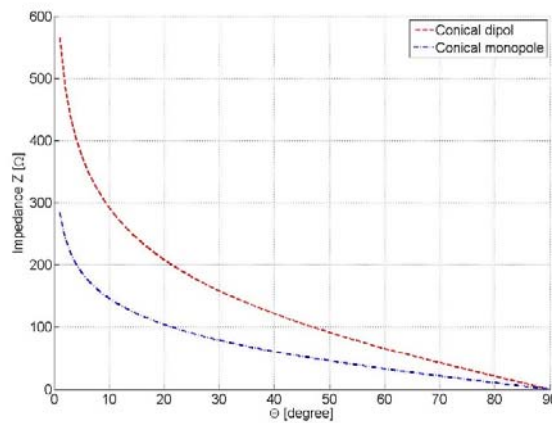

Figure 3.2: Infinite long bowtie antenna impedance for a conical dipole and its corresponding monopole, as a function the angle θ Eq. (3.8)

In order to minimize the radiation losses, a coplanar waveguide (CPW) is used as a feedline structure. Also, because of the infinitesimal feed point of the bowtie monopole antenna, a concatenation approach, according to Figure 3.3 is taken so that both structures can fit geometrically. Since the assumption is that the antenna impedance is not defined by the length of the sides of the bowtie monopole, but rather by their ratio,

correspondingly by the angel θ (Figure 3.2), a simulation optimization of the angle is implemented to find the best achievable match between feedline and radiating element, i.e. half of the bowtie.
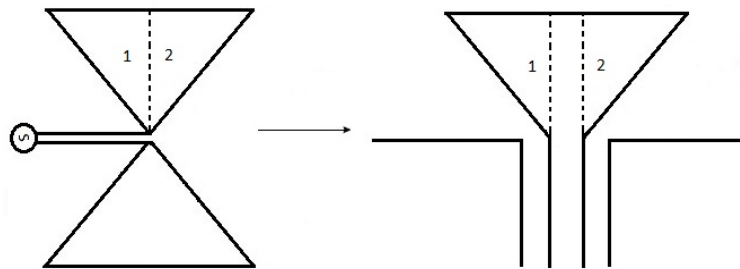

Figure 3.3: CPW and bowtie monopole concatenation (a look from the top)

After optimization simulation (Figure 3.4) of the antenna geometrical parameters, i.e. width ($W = 20.6$ mm) and length ($L = 28$ mm) w.r.t. impedance match and size, an antenna with promising results is realized by photo plotting and chemically etched on a RO4003 substrate with an approximate dielectric constant of $\varepsilon_r = 3.54$ (Figure 3.5).
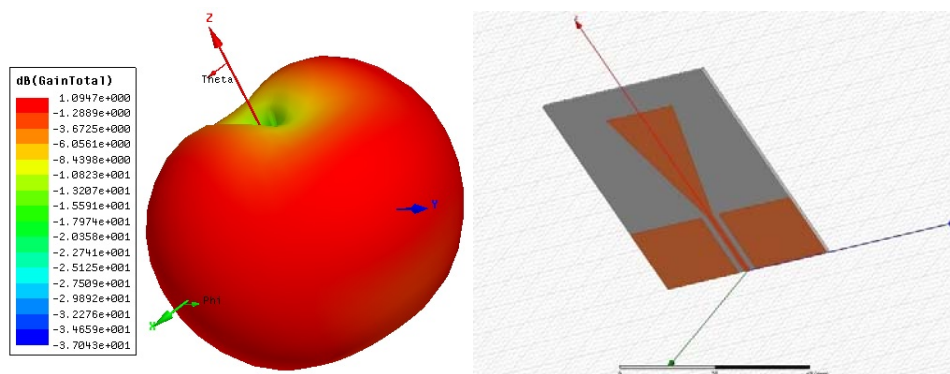

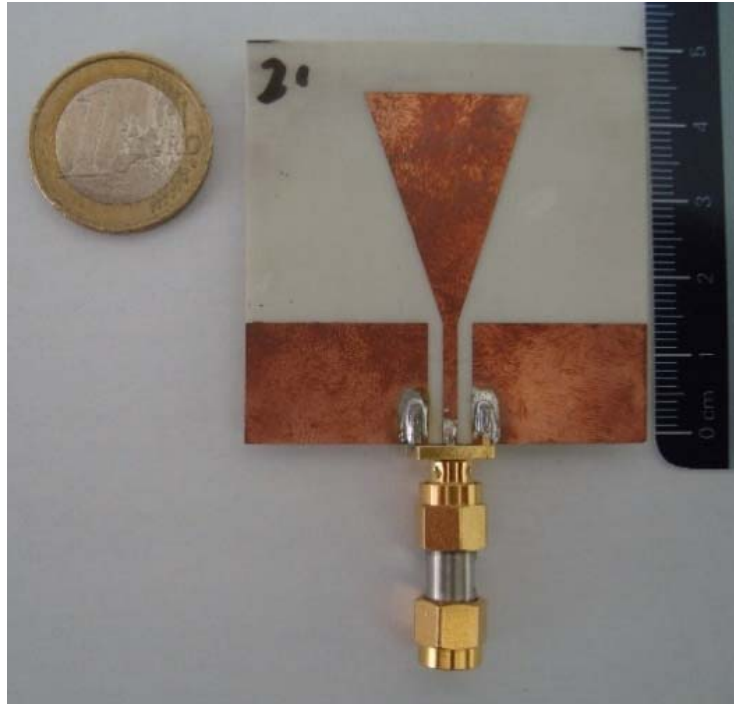Figure 3.4: Simulated antenna 3D radiation pattern at 4 GHz

Figure 3.5:   Realized bowtie monopole antenna

3.4 Bowtie monopole antenna measurements

The following section summarizes the antenna parameters, which are used in the next chapter for the UWB transceiver characterization.

3.4.1 Matching

Figure 3.6 depicts an UWB bandwidth of the antenna w.r.t the mismatch in the range between 3.4 to 4.2 GHz. Compared to the bands of the desired UWB channels (Table 2.2), the antenna is showing a suitable impedance match for UWB channel #2 – approximately, from 3.625 to 4.325 GHz.
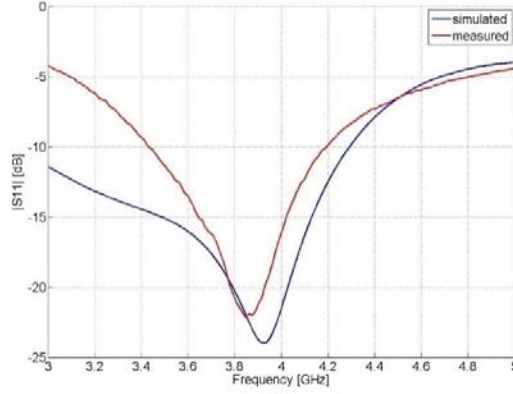
Figure 3.6: Comparison of simulated vs. measured bowtie monopole antenna $|S_{11}|$

parameter

3.4.2 Group delay

The group delay of a single antenna is estimated according to equation 3.9, by measuring the total group delay between the two antennas, subtracting from its value the TOF and dividing it by 2, assuming the two antennas are identical. For convenience the distance between the two antennas is adjusted to 30 cm as this corresponds to approximately 1 ns, which is in the Far field region of each antenna w.r.t. the band from 3.7 GHz to 4.2 GHz.

$$\tau_{antenna\ group} = \frac{\tau_{meas\ group} - \tau_{ToF}}{2}, \quad (3.9)$$

with

$$\tau_{meas\ group} = -\frac{d\varphi}{d\omega}, \quad (3.10)$$

and

$$\tau_{TOF} = \frac{d_{antenna}}{c_0}, \hspace{4cm} (3.11)$$

where $\tau_{meas\ group}$, $d_{antenna}$ and $\tau_{antenna\ group}$ are the measured group delay from the input of one antenna to the output of the other identical antenna, the distance between the antennas and the actual measured group delay for a single antenna, respectively. The measured group delay $\tau_{meas\ group}$ is a calculated by taking the two antennas, facing the same radiation pattern and measuring the phase of the transmission coefficient as a function of frequency, i.e. phase component of S_{21} - parameter. Any consequential negative group delay values are the result of the nonlinear behaviour of the phase (Figure 3.6).
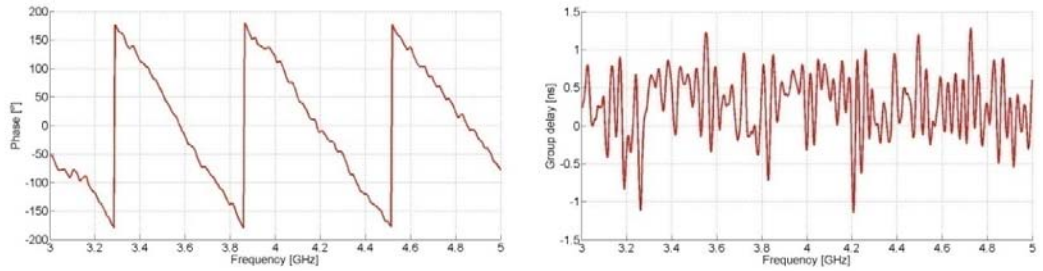

Figure 3.6: $\angle S_{21}$ vs. group delay of the bowtie monopole antenna

CHAPTER 4: Measurement results

This chapter comprises of two main subparts. The first one presents the range estimation measurement results of the UWB transceiver from Chapter 2 in an indoor line of sight (LOS) and "pseudo"-LOS scenario, demonstrating their dependence on the environment and the effect of standard and non-standard compliant transmission parameter settings, such as center frequency, bandwidth, preamble length and bit rate on the ranging accuracy.

The second subpart presents the difference in the group delay between two sets of antennas and their effect on the ranging precision – with and without calibration.

4.1 Test setup

The following measurement results were performed indoors at the Institute of Telecommunications at the Vienna University of Technology (Figure 4.1), where a rich scattering environment is assumed [29]. The part of the hallway considered for the range measurement has the length of 55 meters and the radius in which no obstruction enters the path between transmitter and receiver is 1.3 meters. During each ranging measurement, both nodes have the same configuration of the transmission parameters and are connected to identical antennas and identically oriented towards each other. The range measurement grid, used as a reference does not have the finest precision and a deviation of 4 cm from the ideal range is assumed. The measurement setup comprises of setting the two EVB1000 boards at the aforementioned distance, where 50 consecutive roundtrip time measurements have been carried out (Figure 2.8), calculating the range, based on the TOF, Eq. (2.3).

Figure 4.1: Measurement setup [29]

The results are documented with their statistical first and second order moments, i.e. mean and standard deviation. Unless stated otherwise, the values are defined by the difference between the actual range and the mean from the 50 two-way ranging measurements

$$y = x - \mu_y, \qquad (4.1)$$

where x, μ_y, and y are the actual range, the mean from 50 range measurements, and their corresponding difference, also referred to as the ranging error. The goal is to observe the effect of a single transmission parameter setting on the ranging precision, while keeping the rest of the parameters constant. The effect of the different bit rate, the preamble length, the PRF, signal bandwidth and center frequency parameters are put into perspective to known relations like Friis' transmission equation Eq. (3.4) and LOS communication, where the obstruction free 1st Fresnel zone assumption is met. From now on Fresnel zone is going to be used instead of the term 1st Fresnel zone. The maximum ranging reach is determined up to the point where the cycle-redundancy check

(CRC) error count of the received frame increases up to the point, where the ratio between retransmission, due to CRC error frames, and correctly received frames surpasses 25% and is going to be referred to as "maximum detectable range". Referring back to Chapter 2, the initiator (Tag) is going to remain static, for the ranging measurement setup, whereas the responding node (Anchor) is assuming the role of the range probe. Crucial aspect of the precision of the measurement is the calibration - it is performed by setting the two devices at 7 m distance apart and symmetrically adjusting their preconfigured delays, i.e. changing the delay by the same amount on both devices simultaneously (Figure 4.2).
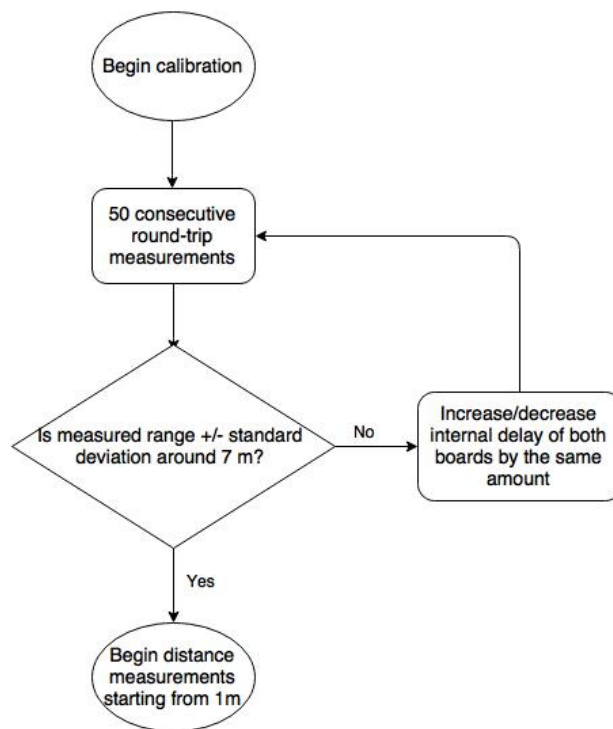

Figure 4.2:   Calibration model

4.2 LOS and pseudo-LOS range scenarios

The first scenario of interest is the case where, there is no obstruction in the line of sight. However, because of the bandwidth of the transmitted pulse and because of the frequency dependence of the Fresnel radius, the range in which the LOS condition is fulfilled, can range up to several meters, depending on the operational band of choice (Figure 4.3), calculated as

$$r = \frac{1}{2}\sqrt{\frac{d\ c_0}{f}}, \tag{4.2}$$

where r, d, c_0, and f are, the Fresnel radius, the distance between the two nodes, the speed of light and the frequency, respectively [30].
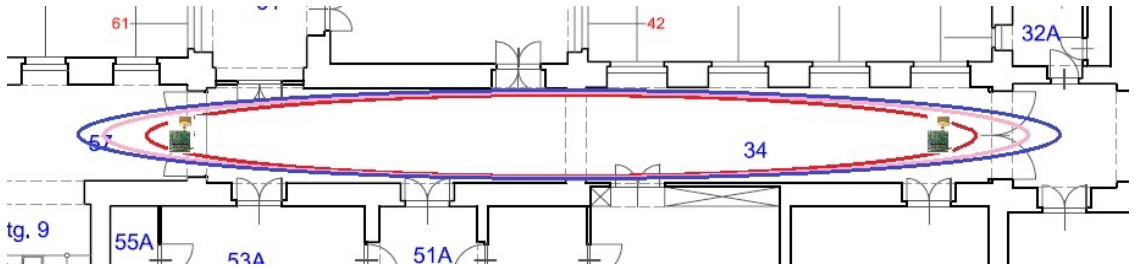

Figure 4.3:   Fresnel zone at operational band #1(red $- f_L$, magenta $- f_C$, blue $- f_H$) [29]

Figure 4.4 summarizes the distance-to-frequency relation for the operational bands (Table 2.2) supported by the UWB chip, given the current indoor ranging measurement environment, where the orange horizontal line represents the radius, after which obstructions start to invade the free Fresnel zone (range threshold), where Table. 4.1 presents, the free Fresnel zone distances for the corresponding operational bands.

Operational band	Max range (m)
Channel 1	17.4 – 19.2 – 20.9
Channel 2	20.1 – 21.9 – 23.7
Channel 3	22.8 – 24.6 – 26.4
Channel 4	18.7 – 21.9 – 25.1
Channel 5	33.8 – 35.6 – 37.4
Channel 7	32.4 – 35.6 – 38.8

Table 4.1:   Ranges up to which the Fresnel zone is free (left $- f_L$, center $- f_C$, right $- f_H$)

The region after the range threshold, where the highest frequency component f_H of a given UWB channel bandwidth reaches an obstruction in its free Fresnel zone is going to be referred to as the pseudo-LOS region. As some of the frequency components of the transmitted signal are obstructed, it is expected, that the ranging performance in that region is going to be inferior. The direct line-of-sight between both nodes, is not obstructed by any means. Nevertheless, a free Fresnel zone is considered as a prerequisite for a LOS transmission. Also, the measurement results do not consider any multipath propagation effects caused by the ground reflection, due to a 180-degree phase shift of the reflected signal. Reflections from the high ceiling are assumed to have a negligible impact on the range measurement.
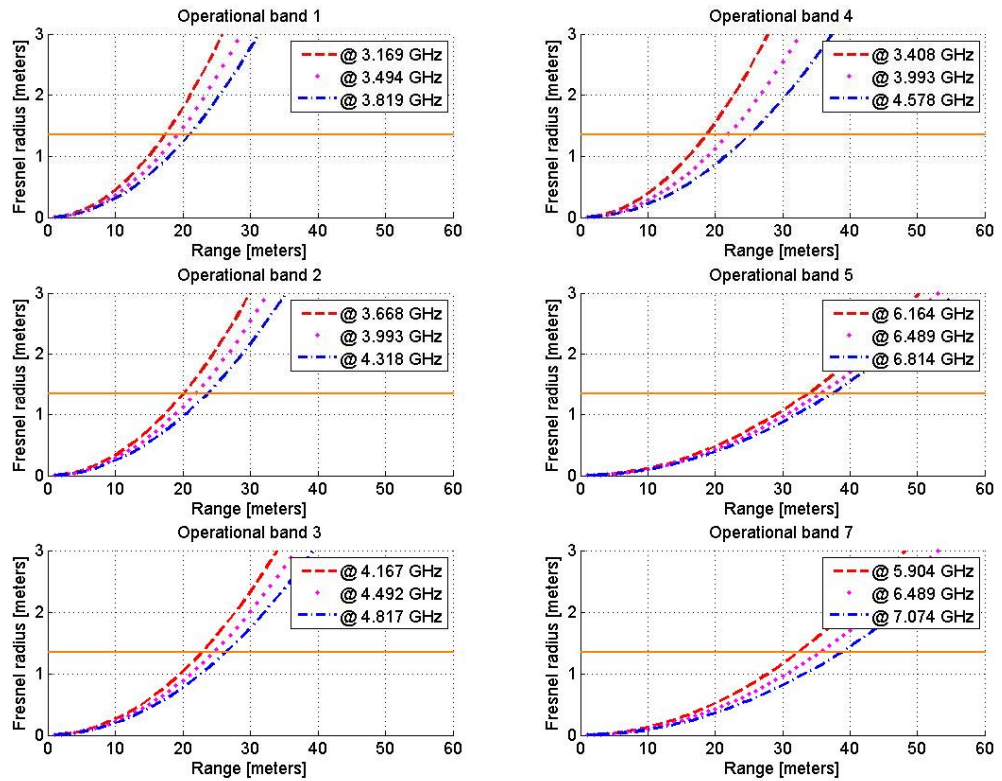
Figure 4.4: Fresnel radius for the IEEE 802.15.4 – 2011 operational bands supported by

the UWB transceiver

4.2.1 Bit rate

When transferring at higher data rates, the transmissions are more frequent in time and so is the average transmitted energy. In order to be conform to the regional regulations and in the case of a higher rate of transmission, the overall transmit power must be lowered, ergo, according to Friis' transmission equation, Eq. (3.4), the achievable range is also lowered. In general, it is assumed, that the increase of the bit rate parameter has a decreasing effect on the maximum detectable range [31]. However, the average transmit

power is measured by the spectrum regulation bodies w.r.t. 1 ms. If the transmission of only one frame takes less than a millisecond, while no other frame is being transmitted within that same interval, the power may be increased, in order to achieve a larger maximum detectable range, while still being conform to the regional spectrum regulation constraints. This consideration is presented by the UWB transceiver as a feature, referred as "Smart Transmit Power Control" [32].

Although, the spectral masks for the three different transmission rates, within the band of interest have relatively the same power spectral densities, the actual transmission power level configured at the 6.8 Mb/s is higher by 6 dB, compared to those at 110 kb/s and 850 kb/s, which is contrary to the theoretical reasoning from the beginning of the previous paragraph.

While keeping the other settings the same and comparing the maximum detectable range, w.r.t. the supported data rates – 110 kb/s, 850 kb/s and 6.8 Mb/s, the range shows as expected, that with increase of the data rate, the maximum detectable range decreases, e.g. the range at 6.8 Mb/s decreases down to 41 meters, where for the lower data rates, the maximum range is either at or beyond the scope of the measurement grid (Figure 4.5).

The effect of the increase of the bit rate on the ranging error, on the other hand, is questionable:

- For the LOS range region, the difference between ranging estimation results at 110 kb/s and 850 kb/s is lower than 3 cm and comparing both of them to the ranging estimation at 6.8 Mb/s, gives a maximum difference of 5 cm.

- The difference for the pseudo-LOS region – comparing 6.8 Mb/s with the other two bit rates, reaches 7cm and when the lower bit rates get compared – a maximum deviation between each other of 4 cm has been reached.
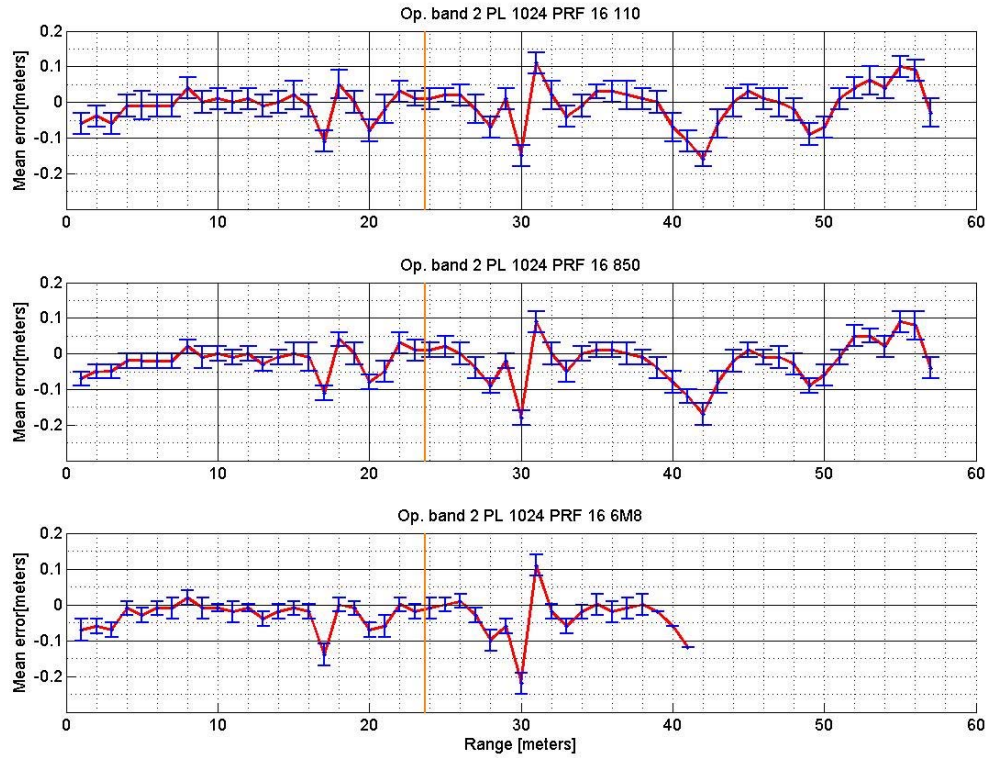

Figure 4.5:   Comparing different bit rates at operational band #2

4.2.2 Centre frequency

From Friis' link power budget equation Eq. (3.4), the free-space path loss (FSPL) equation is formulated as:

$$FSPL/dB = 20\ log_{10}d + 20\ log_{10}f + 20\ log_{10}\frac{4\pi}{c_0},\qquad(4.3)$$

where d, f, and c_0 are the distance between the transmitter and the receiver in meters, the frequency in Hertz and the vacuum speed of light in meters per second, respectively. The above equation implies that the transmission at higher frequencies experience higher propagation losses, so transmitting at lower frequencies should maximize the transmission range.

As plotted in Figure 4.6, with increase of the frequency, there is an inconsistent decrease in the maximum detectable range, at which the receiving node can receive frames, where all the other transmission parameters are configured the same. At operational band #3, i.e. a center frequency at approximately 4.5 GHz, there is a significant increase in the maximum reached range, compared to transmission at approximately 4 GHz , or even at approximately 6.5 GHz, which is not follow the path loss formula above.

However, regarding the ranging error, there is an increase in the mean ranging error, as the measured range surpasses the Fresnel free threshold, indicated by the orange marker:

- For the LOS range region, the range error is in the range of around 10 cm respectively, which is consistent with the margin specified by the manufacturer in Sub-chapter 2.2.

- For the pseudo-LOS region, where only the lower group of bands, i.e. below 5 GHz surpass the "ideal"-LOS threshold and the maximum range error reaches 33 cm, 22 cm and 15 cm, for the operational bands #1, #2 and #3, respectively.
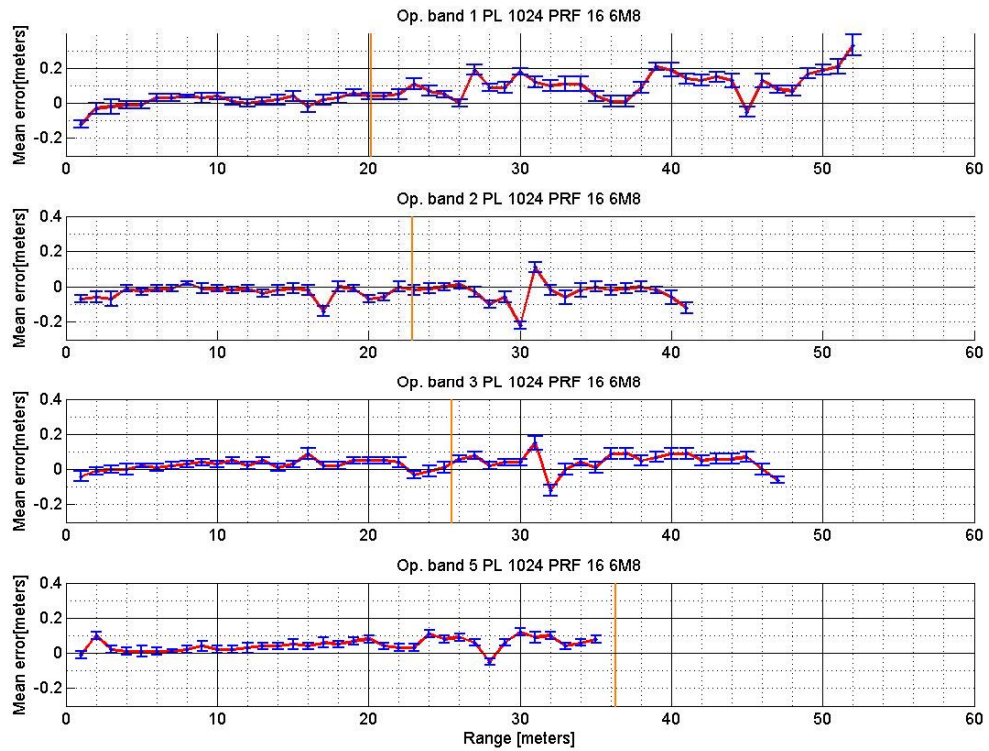
Figure 4.6: Range error mean and standard deviation at operational bands #1, #2, #3 and #5

4.2.3 Bandwidth

Another way to improve the maximum range is by using the bands, which occupy larger bandwidth, i.e. 900 MHz instead 500 MHz, as this implies larger amount of transmitted energy. As stated in the introduction, larger bandwidth also implies that the temporal resolution of the symbols is more precise, which is assumed to be beneficial for the ranging precision. As it can be seen from Figure 4.7, the mean error can be considered constant at different ranging sectors. For example, the absolute average range error at operational band #4 from the 20th to the 36th meter is 21 cm and from 37 till the end is

43

47 cm. Similarly, for the operational band #7 – from the 10th meter till the end the absolute average range error is 21 cm. According to the measurements the LOS threshold does not have an impact on the ranging error.
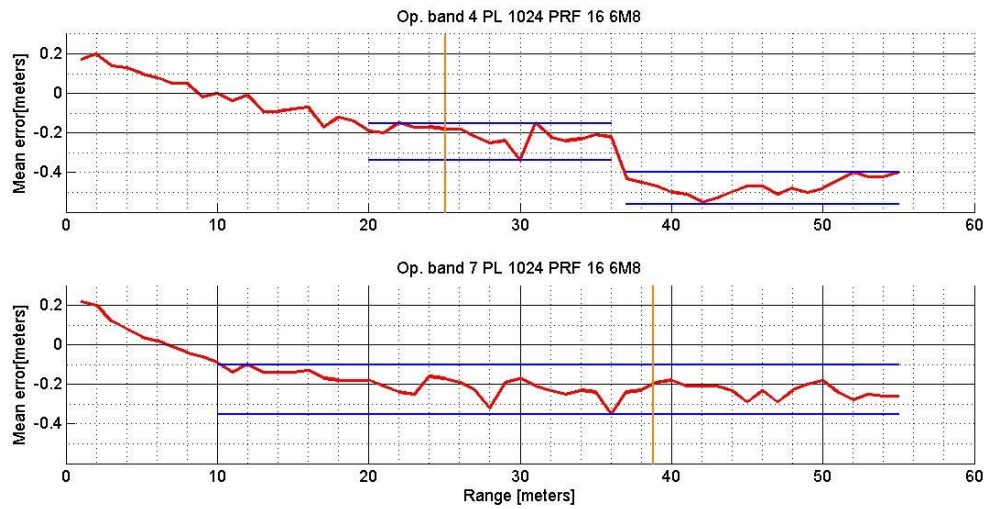
Figure 4.7: Comparing ranging precision at 900 MHz bandwidth for operational bands #4 and #7

4.2.4 Pulse Repetition Frequency

It is assumed that a 64 MHz PRF results in more precise range estimation on first path timestamp and might lower the ranging error compared to 16 MHz. This statement could neither be confirmed nor denied by the measurement results (Figure 4.8). The ranging error for both PRF values reaches a ranging error of at most 12 cm.
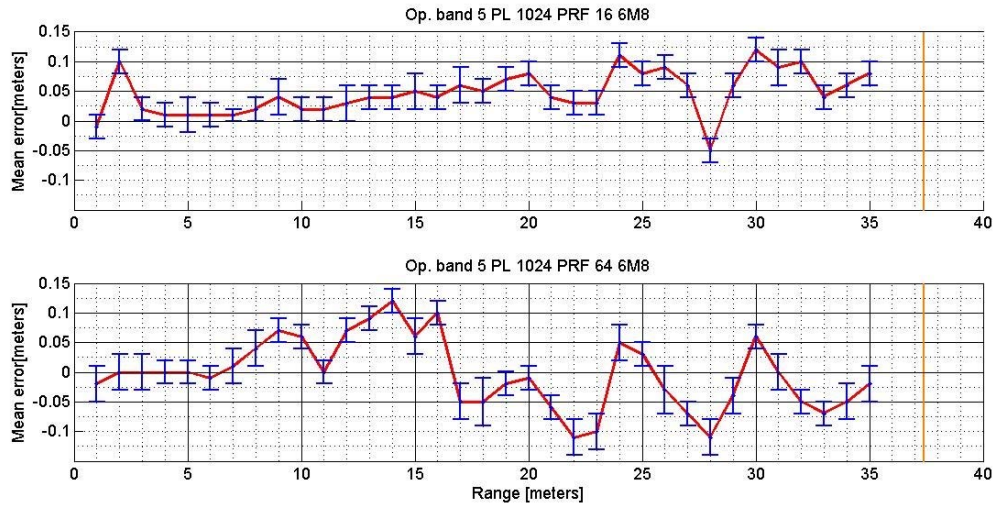
Figure 4.8:   PRF 16 MHz(up) vs. 64 MHz(down) comparison

4.2.5 Preamble Length

As mentioned in Sub-chapter 2.1, the IEEE standard preamble lengths are 64, 1024 and 4096 and their performance is compared to the non-standard values, supported by the UWB transceiver. The preamble length is assumed to have an impact on the timestamp precision and given the same transmit power, the preamble length in conjunction with the bit rate has an impact on the overall power spectral density.

Transmission at low data rate – 110 kb/s, with the shortest achievable preamble length of 64 symbols is considered nonsense, as proven by the range measurement, where the CRC error count is high even at a range of 1 meter and the UWB frame transmission is constantly interrupted. However, if we take for comparison, the same data rate and doubling the preamble length results in the increase of the power spectral density

45

approximately by 6 dB at the center frequency, by 6 dB at the -10 dB marker and by 4 dB at the -18 dB marker. On the other hand, higher data rates with a too long preamble length can be considered useless, if it does not improve the ranging precision [33].

The assumption, that the highest precision can be achieved at the highest achievable preamble length, i.e. 4096 preamble symbols, is not supported by the results in Table 4.2, where all the achievable preamble lengths and bit rate combinations at operational band #2 have been compared with the highest preamble length and where all other transmission parameters are the same Eq. (4.5).

Preamble length	LOS	pseudo-LOS	Total
64	n/a / 0.43 / 1.74	n/a / 3.67 / 1.94	n/a / 2.09 / 1.83
128	1.61 / 1.17 / 0.22	0.16 / 0.58 / 0.28	0.58 / 0.28 / 0
256	1.22 / 1.52 / 1.7	0.91 / 0.12 / 1.83	1.04 / 0.81 / 1.76
512	3.48 / 2.57 / 5.04	2.91 / 1.04 / 4.78	3.15 / 1.79 / 4.93
1024	0.13 / 1.87 / 0	0.69 / 1.08 / 4.61	0.45 / 1.47 / 4.27
1536	1.13 / 2.35 / 4.57	1.44 / 1.21 / 3.44	1.31 / 1.77 / 4.07
2048	0.22 / 2.04 / 3.13	1.16 / 1.29 / 3.94	0.58 / 1.66 / 3.49

Table 4.2:   Average of the absolute difference of the different preamble length (in cm) measurements compared to preamble length of 4096 in cm Eq. (4.5), at different bit rate transmissions – 110kb/s (left) / 850 kb/s (middle) / 6.8 Mb/s (right)

The difference in ranging error between different preamble lengths is within the standard deviation for most of the mean range errors, which is 3 cm and above 4 cm for only few of the range measurements.

$$\Delta y \ = \ y_{PL\,max} - \ y_{PL} \, , \qquad\qquad (4.5)$$

where $y_{PL\,max}$, y_{PL} and Δy are the measured mean range error for preamble length of 4096, the measured mean range error for any other preamble length and their difference, respectively. Except the assumed maximum detectable range increase, there is no significant improvement in the precision of the ranging estimation between different preamble lengths.

4.2.6 Custom mode

The EVB1000 gets delivered with a set of pre-calibrated delay values and transmission settings (or modes) stored in the accompanied microcontroller, where the modes use a non-standard SFD [34]. Under the same transmission parameters, the range measurements of mode 3 ($y_{factory\,def}$) configured nodes get compared with those of locally calibrated nodes ($y_{local\,cal}$), where the depicted difference (Δy) shows a significant increase the ranging error (Figure 4.9)

$$\Delta y = y_{local\,cal} - y_{factory\,def} \qquad (4.6)$$

The percentage of the range error for the locally calibrated measurements for the error segments between 5 and 10 cm, and above 10 cm, w.r.t. the LOS and the pseudo-LOS regions are 17/4% and 19/16%, respectively. This leads to the conclusion, that a local calibration is essential, if a higher level of precision, i.e. lower ranging error is a requirement.

4.3 Bowtie monopole comparison

The current section compares the range measurements done with the bowtie and the elliptical monopole antennas, in conjunction with a calibrated and non-calibrated

transceiver. The presented statistics are a result of a set of range measurements that are implementing a comparison model, that tests, whether the difference in internal delay calibration between measurements with two different sets of antennas, can be compensated manually by the average antenna group delay, without the need of additional calibration.
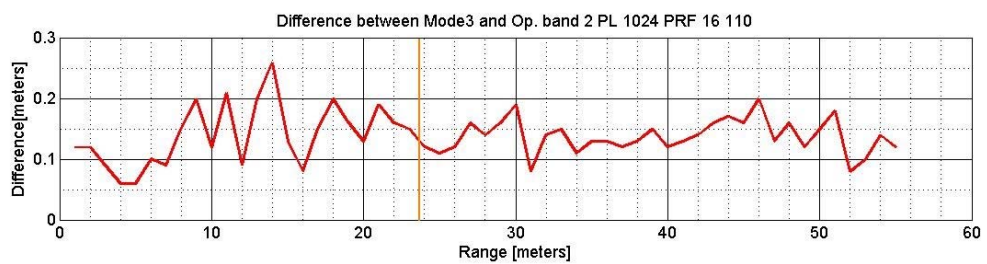

Figure 4.9:   Comparison between EVB1000 mode3 and a locally calibrated range measurement Eq. (4.6)

4.3.1 Antenna group delay comparison

In order to compare the effect of the difference in group delay of both antennas on the ranging precision, two sets measurements with the same transmission parameters and same EVB1000 internal delay values are made with elliptical and bowtie monopole. In addition to them, a third range measurement is performed with an internal delay values, calibrated with the bowtie monopole. The UWB transceiver is calibrated for the bowtie monopole antenna, by changing the internal delay value for the elliptical antenna calibration by the same amount at both transmitter and receiver. By making the change in this manner, the difference between the two internal delay values for the two different calibrations, i.e. for the elliptical and bowtie monopole antenna sets, will be the same for

the transmitter and the receiver. In total, 3 ranging measurements are done, with the same transmission settings – two calibrated and one non-calibrated (Figure 4.10).
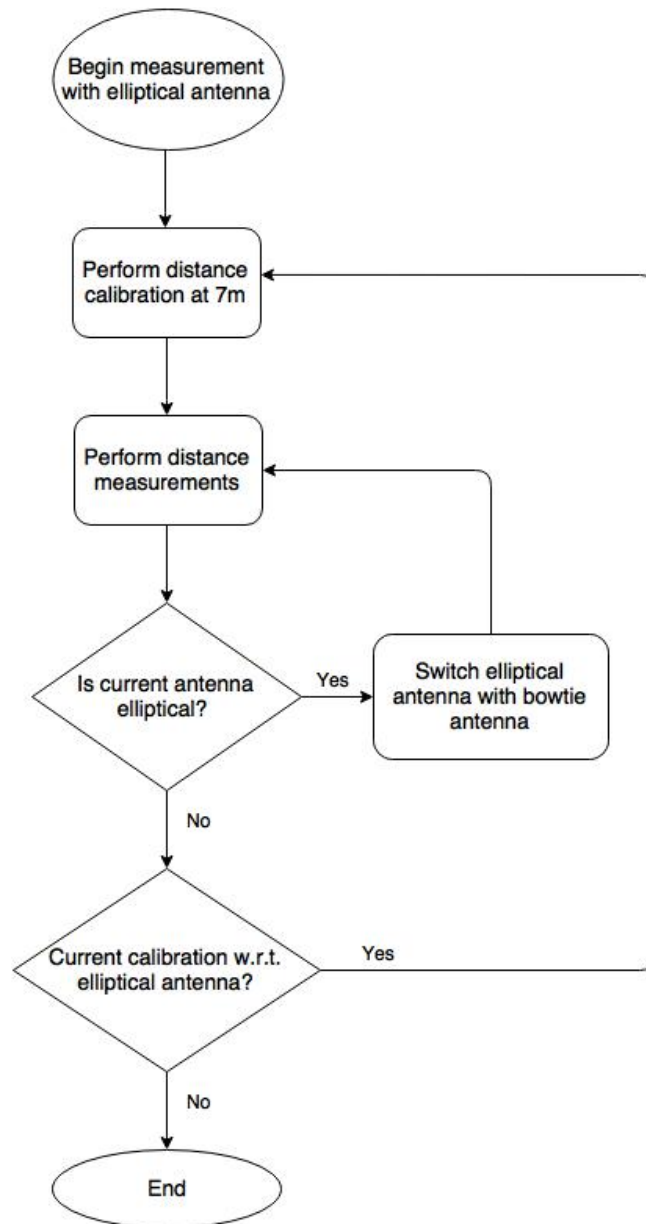

Figure 4.10:   Bowtie vs. Elliptical monopole antenna range estimation comparison

	Elliptical	Bowtie	Δ
Mean group delay (in ns)	0.24	0.28	0.04
Effective delay distance (in cm)	7.2	8.4	1.2

Table 4.3: Average antenna group delay vs. effective delay distance for operational band #2

Comparing the averages of the group delays Eq. (3.10) of both elliptical and bowtie monopoles, w.r.t. the corresponding operational channel bandwidth, shows that the bowtie monopole has a bigger value of the average group delay compared to the elliptical.

$$\Delta t \ = \ t_{AD\ bowtie\ cal} - \ t_{AD\ elliptical\ cal} \qquad (4.7)$$

The difference in EVB1000 internal delay Eq. (2.4), w.r.t. the calibration of the elliptical and the bowtie monopole, is depicted in Table 4.3.

Preamble length	Δt @110 kb/s (in ns)	Δt @850 kb/s (in ns)	Δt @6.8 Mb/s (in ns)
64	n/a	0.37	0.19
128	0.08	0.14	0.31
256	0.21	0.14	0.19
512	0.11	0.13	0.19
1024	0.275	0.15	0.22
1536	0.13	0.15	0.22
2048	0.13	0.15	0.22
4096	0.13	0.15	0.22

Table 4.4: Difference of internal delays between an elliptical and bowtie monopole antenna calibrations Eq. (4.7)

, where the difference in the internal delays at the transmitter (t_{ADTX}) and at the receiver (t_{ADRX}) is the same, because of the chosen calibration model (Figure 4.3), and where measurements were performed for UWB operational band #2.

$$\Delta t = t_{AD\ bowtie\ cal} - t_{AD\ elliptical\ cal} \qquad (4.8)$$

Comparing the antenna group delay (Table 4.3) values with the difference in EVB1000 internal delays, for both calibrated measurements and for both antennas (Table 4.4), results show that the mean antenna group delay for operational band #2 differs in the order of a magnitude from the internal delay value Eq. (4.8). This suggests that the calibration process cannot be skipped, if there is the need for antenna change and group delay measurement is inconsistent with the value of the transceiver delay.

4.3.2 Effective delay distance

Following the speed of light-to-distance relation Eq. (2.6), the time delay values can correspondingly be expressed as equivalent "effective delay distances": at the -10dB bandwidth mark, a mean delay difference of 0.04 ns corresponds to 1.2 cm effective delay distance (Table 4.3).

The histograms in Figure 4.11 are presenting the statistical relations between calibrated range measurements of both antenna types. The emphasis is on the difference between precision in the LOS and the pseudo-LOS regions. In addition, due to the fact that the LOS threshold for operational band #2 does not split the ranging grid in two equal in length halves, the sample space for the LOS case is 529, while for pseudo-LOS - 621. The results show that for the calibrated measurements with the elliptical antenna, in the

LOS scenario – 20 % of the cases present a range error between 10 cm and 5 cm and 78 % - bellow 5 cm and only 2% above 10 cm.
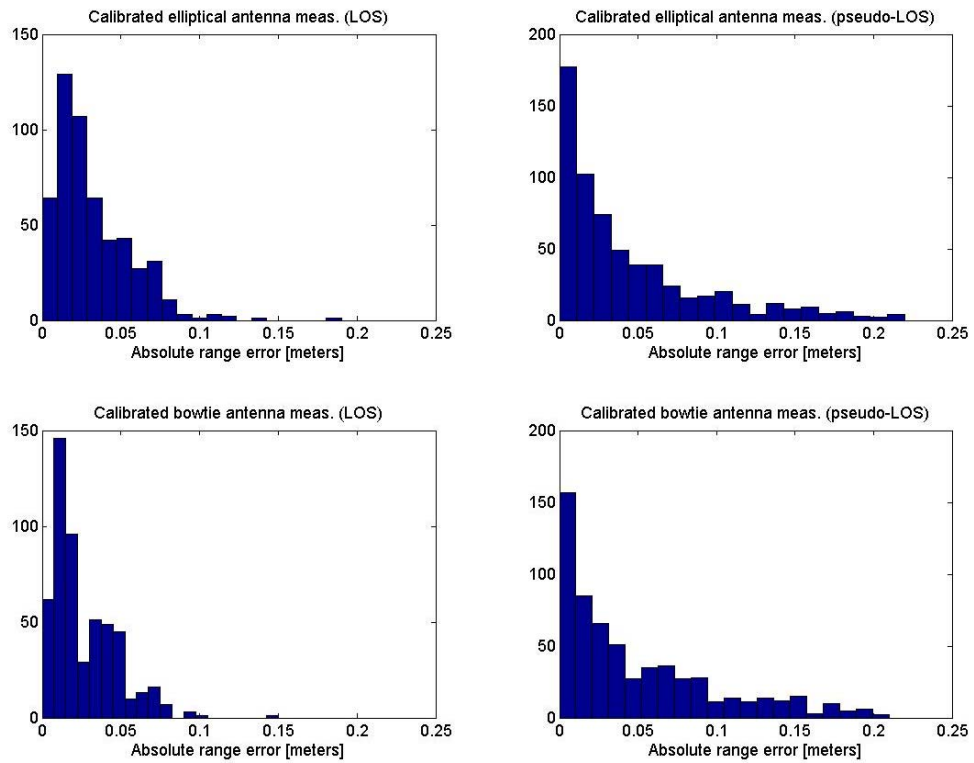

Figure 4.11:   Histogram of the calibrated measurements for both elliptical (up) and bowtie (down) monopoles for the LOS (left) and pseudo-LOS (right) regions

Despite the expectations for inferior performance in the pseudo-LOS region, the statistical results of the ranging precision still show, that in 69% of the cases, the ranging error is below 5 cm, 17 % - is between 5 and 10 cm and 14% above 10 cm. The calibrated measurements for the custom, bowtie monopole antenna show rather similar behavior results, where within the LOS region 16 % of the cases lie below the 5 cm mark, 83 % are between 5 and 10 cm and less than 1 % - above 10 cm. The interpretation of the mean

and the first mode show misleading results, as the first moment for both antennas is at 2 cm, while the mean value varies between 3 and 5 cm, for the four different histograms above. In total (histogram not shown), for all the calibrated ranging measurements with, two different antennas - 91% of the cases shown a ranging error bellow 10 cm.
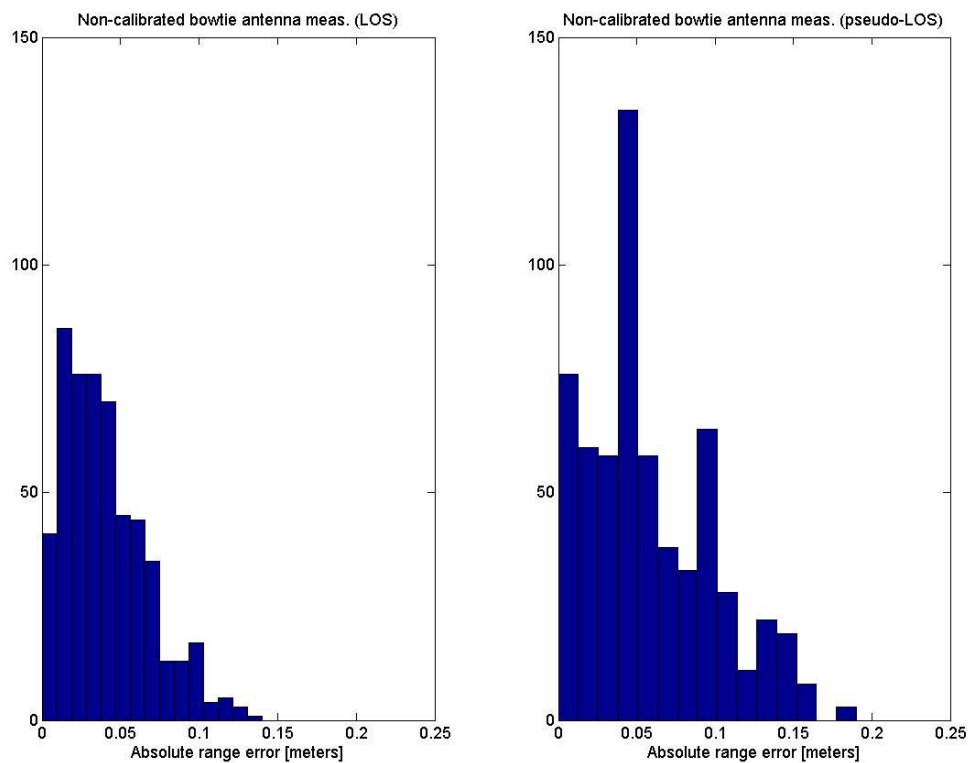

Figure 4.12:   Histogram of bowtie monopole range measurements with internal delay calibration settings for an elliptical antenna for the LOS (left) and pseudo-LOS (right) region

Comparing the histogram of the calibrated range measurement (Figure 4.11) to the statistical plot of the non-calibrated measurements (Figure 4.12), i.e. measurements done with a bowtie monopole antenna with an EVB1000 transceiver, calibrated for an elliptical

antenna, does not show a distinguishable 1st-mode offset on the histogram for the LOS scenario. This can be explained by the too low difference in the mean group delay between both antenna sets. However, the pseudo-LOS histogram depicts an offset of the 1st mode of 4 cm – this is in the order of 2.5 times bigger offset, compared to the calculated effective delay distance, but close to the average internal delay value w.r.t. Table 4.4.

CHAPTER 5: Summary

The ranging precision of an off-the-shelf commercial ultra-wideband transceiver has been tested based on indoor measurements carried out with two sets of UWB antennas. A dedicated UWB Bow Tie antenna was designed, manufactured, and characterized. The goal was to evaluate the quantitative effects of various transmission parameters and connected UWB antennas on the ranging precision.

5.1 Conclusion

Since only one sensor node was used for the measurement, only the *ranging* precision was evaluated. However, the nodes used for the measurements are evaluation boards (EVK1000 = 2 x EVB1000) supplied by constant voltages from stable power supplies. The measurements are a result of a continuous acquisition process, where the UWB sensor chip does not switch into a low-power sleep mode between transmissions and the power source is considered long-term stable. This is a somewhat idealized measurement scenario unlike a battery powered node. As for a real-world mobile node, these ideal conditions are unlikely to be met. The power usage is a consideration, where power refers to the transmit power, but also for processing power of the controlling microprocessors' firmware.

Measuring the chips' performance as part of a custom, low scale battery powered solution decreases the time in which the transceiver behaves stably, i.e. one has to take into account much more sources of instability:

- Drift in the oscillator during start-up

- Drift in the internal time clock

- Drift in temperature

The presented results lead to the following conclusions, under the assumption for a continuous transmission of the transceiver:

- A direct relation between the difference in antenna mean group delay and the device's calibrated internal delay was not proven.

- Additional delay calibration is essential for achieving a ranging error smaller than 10 cm for a large percentile of all cases.

- A consistent ranging error below 10 cm is achievable in the "ideal"-LOS region.

- With decrease of the data rate, there is an increase of the achievable transmission range. Outside of the "ideal"-LOS region, the ranging precision degrades.

- Increasing the preamble length does not have any significant impact on the ranging precision.

- Increasing the pulse repetition frequency did not show any impact on the ranging precision.

- A straightforward relation between the transmission signal bandwidth and the ranging error was not observed in the measurements.

5.2 Suggestions for future work

Despite the promising results in ranging precision, there several aspects that can be further investigated:

- Performing a range measurement comparison between antenna sets with significant difference in the average group delay – this way the effect of the group delay may be observed more distinguishably in the statistical sense.

- The custom designed bowtie monopole antenna is an electrical monopole and the transceiver SMA port is positioned in such a way that the dielectric, PCB board lies within the Near field of the antenna. A better approach towards antenna design for embedded applications is to realize a magnetic antenna.

- Another possible improvement towards increase in the precision is to implement a better ranging algorithm such as symmetric double-sided two-way ranging, where both sensor and probe are separately initiating the ranging and each side is calculating the TOF, w.r.t. its own internal processing delay. Also, an investigation on the possible decrease in ranging precision can be considered the other way around – by determining the distance from the transmission of only one UWB frame roundtrip, i.e. one-way ranging.

- Finally, it is worth mentioning that the UWB chip provides some degree of freedom, by deviating from the IEEE 802.15.4 – 2011 standard and it should be

considered if, for example a custom designed Start of Frame Delimiter (SFD) would improve the ranging precision.

REFERENCES

[1] OSD/DARPA Ultra-Wideband Radar Review Panael, "Assessment of Ultra-Wideband (UWB) Technology," pp. 1 to 9, 13 July 1990

[2] I. Oppermann, M. Hämäläinen, J. Iinatti, "UWB Theory and Applications," pp.5, 2004

[3] F. Hlawatsch, "Information Theory and Coding," Lecture notes, pp. 5 to 14, October 2011

[4] A. F. Molisch, "Wireless Communications," 2nd Edition, pp. 102 – 105, 2011

[5]   J. Randy Hoffmann, M. G. Cotton, R. J. Achatz, R. N. Statz, "Addendum to NTIA Report 01-384: Measurements to Determine Potential Interference to GPS Receivers from Ultrawideband Transmission Systems," pp. vii to xi, 2001

[6] Revision of Part 15 of the Commission's Rules Regarding Ultra-Wideband Transmission Systems, "First Report and Order" pp. 2 to 26 and pp. 103 22. April 2002

[7] U.S. Government Publishing Office, "Electronic Code of Federal Regulations, Title 47, Chapter |, Subchapter A, Part 15, Subpart F—Ultra-Wideband Operation," §15.503, 8. September 2016

[8] ETSI Technical report, "Short Range Devices (SRD) using Ultra Wide Band (UWB); Technical Report Part 1: UWB signal characteristics and overview CEPT/ECC and EC regulation", ETSI TR 103 181-1 V1.1.1 (2015-07), pp. 18, July 2015

[9]   RTL Service Real Time Location Systems, RealTrac(TM) Technology the real-time positioning system, http://rtlservice.com/en/solutions/manufacture/, August 2016

[10]   J. Jung, D. Kang, C. BaeI, "Distance Estimation of Smart Device using Bluetooth," CSNC 2013 : The Eighth International Conference on Systems and Networks Communications, September 2016

[11]   O. Hernandez, V. Jain, S. Chakravarty and P. Bhargava, "Position Location Monitoring Using IEEE 802.15.4/ZigBee technology," NXP

[12] "Popai's 2014 Mass Merchant Shopper Engangement Study - Media Report," POPAI – The Global Association for Marketing Retail, 2014

[13] D. Dodge, "Google Keynote: Why Indoor Location Will Be Bigger than GPS or Maps", 21. November 2013

[14] IEEE Standards Association, "IEEE Standard for Local and metropolitan area networks – Part 15.4: Low-Rate Wireless Personal Area Networks (LR - WPANs)," pp. 194 - 215, 5. September 2011

[15] DecaWave Ltd., "DW1000 Data Sheet," v. 2.02, pp. 5 – Figure 1, 2014

[16] DecaWave Ltd., "DW1000 User Manual," v. 2.02, pp. 101 – 105, 2014

[17] DecaWave Ltd., "DecaRanging (PC) User Guide," v. 2.3, pp. 17 -23, 2014

[18] DecaWave Ltd., "EVK1000 User Manual," v. 1.12, pp. 6 , 2014

[19] DecaWave Ltd., "APS014 Application note; Antenna delay calibration of DW1000-based products and systems," v. 1.01, pp. 3, 2014

[20] DecaWave Ltd., "DW1000 User Manual," v. 2.02, pp. 98, 2014

[21] DecaWave Ltd., "DW1000 User Manual," v. 2.02, pp. 210, 2014

[22] DecaWave Ltd., "APH0007 Application note; Antenna Selection / Design Guide," v. 1.00, pp. 4 -5, 2014

[23] J. Foerester, et.al, "UWB Channel Model Contribution from Intel," pp. 3, 24. June 2002

[24] H. Schantz, "The Art and Science of Ultrawideband Antennas," 2nd Edition, Chapter 3, 2015

[25] O. Lodge, "Electric telegraphy", US609154A, 16. August 1898

[26] J.D. Kraus, "Antennas", 2nd Edition, pp. 340 - 347, McGraw-Hill 1988

[27] Bow Tie Antenna,

http://www.antenna-theory.com/antennas/wideband/bowtie.php, February 2016

[28] Bowtie Antenna Designer, http://www.changpuak.ch/electronics/Butterfly-Antenna-Designer.php , February 2016

[29] Gusshausstrasse 25, 1040 Vienna, CF02 – sections 34, 26, 16, http://www.gut.tuwien.ac.at/fileadmin/t/lm/Plaene/Code_CA_-_CI/CFGHI/F02_G03.pdf , July 2016

[30] C. F. Mecklenbräuker, G. Lasser, „Wellenausbreitung," – Lecture notes, 9. Auflage, pp. 107 – 108, September 2011

[31] DecaWave Ltd., "DW1000 User Manual," v 2.02, pp. 193, 2014

[32] DecaWave Ltd., "DW1000 User Manual," v 2.02, pp. 101, 2014

[33] DecaWave Ltd., "DW1000 User Manual," v 2.02, pp. 194, 2014

[34] DecaWave Ltd., "EVK1000 User Manual," v 1.11, pp. 10, 2014